Published by Avanti Publishers

Journal of Advances in Applied & Computational Mathematics

ISSN (online): 2409-5761

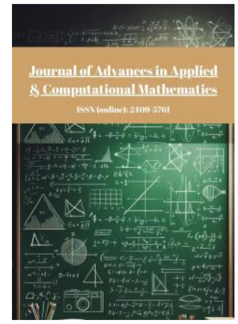

An Efficient Laplace-Adomian Decomposition Approach for a Fractional-Order SIR Epidemic Model with Two Interacting Groups

Hilal G. Yıldız[1] and Hatıra Günerhan[2,*]

[1]*Department of Mathematics, Faculty of Science and Letters, Kafkas University, Kars, Türkiye*

[2]*Department of Mathematics, Faculty of Education, Kafkas University, Kars, Türkiye*

ARTICLE INFO

Article Type: Research Article

Academic Editor: Rajesh Kumar Gupta

Keywords:
Epidemic modeling
Nonlinear dynamics
Fractional SIR model
Caputo fractional derivative
Laplace adomian decomposition method (LADM)

Timeline:
Received: May 10, 2026
Accepted: June 16, 2026
Published: June 26, 2026

Citation: Yıldız HG, Günerhan H. An efficient laplace-adomian decomposition approach for a fractional-order SIR epidemic model with two interacting groups. J Adv Appl Computat Math. 2026; 13(1): 90-104.

DOI: https://doi.org/10.15377/2409-5761.2026.13.6

ABSTRACT

This study examines a nonlinear SIR epidemic model to characterize the dissemination of infectious diseases through a modified version of the Caputo fractional derivative. The Laplace Adomian Decomposition Method (LADM) is used to find both analytical and approximate-analytical solutions for the proposed model. The answers are given as rapidly converging series.

We get approximate analytical solutions that show quick convergence and accurately describe how the system works. The method's reliability has been confirmed, and the proposed fractional-order model's validity has been confirmed.

*Corresponding Author
Email: gunerhanhatira@gmail.com
Tel: +(90) 5013376636

1. Introduction

Mathematical epidemiology frequently employs state-transition models to examine the dynamics of infectious diseases within a population. Such models provide a systematic framework for analyzing the spread and transmission of disease by representing the transition of individuals between different epidemiological states. For example, the Susceptible-Infected-Recovered (SIR) model is one of the most fundamental approaches in this field [1]. However, classical integer-order models typically overlook memory effects and non-local dynamics specific to many real-world epidemiological processes. To address these shortcomings, fractional-order derivatives come into play, modeling disease behavior in a more complex yet realistic manner by incorporating past data, thereby improving prediction accuracy [2]. In this context, a nonlinear fractional SIR model based on the Caputo derivative is being investigated, taking into account memory and hereditary effects commonly encountered in disease processes [3]. The use of fractional-order derivatives enables the modeling of infectious disease dynamics with non-local interactions, offering richer analytical capabilities compared to traditional integer-order models. While traditional models typically assume instantaneous transitions, they neglect the impact of past events on current states. In contrast, fractional-order models incorporate memory effects within the temporal context, enabling a more comprehensive and accurate representation of epidemiological processes [4]. In particular, this approach allows for modeling situations where the rate of change in a compartment depends on past states, thereby revealing hidden aspects of disease dynamics [5]. In this study, both numerical and analytical solutions are derived to analyze the existence and singularity conditions of the fractional SIR model using advanced mathematical methods [6]. Additionally, to understand the long-term behavior of the epidemic, the stability of disease-free and endemic equilibrium points is evaluated in detail under various conditions [7]. Recent studies have significantly expanded the scope of the classical SIR model by integrating fractional dynamics, data-driven approaches, and generalized transmission mechanisms. Taghvaei et al. proposed a fractional SIR framework in which the infection term is modified using a power-law structure, allowing the model to capture heterogeneous contact patterns more realistically [8]. Alqahtani developed a fractional-order SIR model tailored to COVID-19 dynamics, demonstrating that memory effects can substantially influence recovery and transmission rates [9]. Mousa and Alsharari presented a numerical comparison of fractional SIR models, focusing on stability and accuracy of different computational schemes [10]. Qazza and Saadeh introduced an analytical approach based on Laplace transform techniques to obtain approximate solutions of fractional SIR systems [11]. Alazman et al. investigated the role of diffusion and generalized fractional operators in SIR dynamics, showing how spatial and memory effects jointly impact disease spread [12]. Prodanov D. explored nonlinear approximation techniques, including exponential series expansions, to improve the solvability of SIR-type models [13]. Murph et al. focused on parameter estimation and peak infection mapping, highlighting the importance of accurate data fitting in SIR-based forecasting [14]. Shafqat et al. combined fractional SIRD models with deep learning methods to enhance predictive performance in epidemic modeling [15].

In this research, we are also exploring the potential of using the Laplace Adomian decomposition method (LADM) to solve the fractional SIR epidemic model. This method is a powerful yet straightforward approach to tackling epidemic models and has been successfully applied in biology, engineering, and applied mathematics. It combines the Laplace transform and the Adomian decomposition method, offering several advantages for solving complex problems. One of the advantages of this method is its accuracy, as by employing the Laplace transform, it transforms the differential equations into algebraic equations, which are often easier to solve. This transformation reduces the complexity of the problem and enables the use of powerful algebraic techniques to obtain accurate solutions. Additionally, the Adomian decomposition method provides a systematic and robust approach to handling nonlinear terms, allowing for accurate approximation of the solution even in the presence of nonlinearity. This method does not require any perturbation or linearization, nor does it need a defined size of the step like the Rung-Kutta of order 4 technique. Various models have already been solved using this particular technique, such as HIV infection of CD4+ T cells model [16], fractional-order smoking model [17], epidemic childhood diseases [18], Radhakrishnan–Kundu–Lakshmanan equation [19], Asian option pricing model [20], Burger's equation [21], Chen-Lee-Liu equation [22], prey-predator model [23], nonlinear fractional smoking mathematical model [24], HIV model [25], Smoking epidemic model [26], fractional-order COVID-19 model [27].

The novelty of the present study is threefold. First, unlike most earlier fractional-order SIR studies, which treat a single homogeneous population, model (2.1) couples two interacting susceptible-infected-recovered sub-groups through explicit cross-transmission coefficients ξ_{12} and ξ_{21}, so that heterogeneous mixing between two groups can be captured within a single fractional-order framework. Second, this particular two-group model, with its specific combination of recruitment, natural-death, disease-induced-death and recovery terms, has not previously been solved by the Laplace Adomian Decomposition Method. Third, we provide a systematic comparison between the LADM series solution and the classical fourth-order Runge–Kutta (ODE45) solution for $\alpha = 1$, together with a discussion of how $\alpha = 0.75$ and $\alpha = 0.5$ alter the epidemic dynamics of both groups. To the best of our knowledge, this two-group fractional SIR model has not been solved by LADM elsewhere, which constitutes the main contribution of this work.

2. Model Formulation

In this study, we consider the following SIR model with fractional derivatives of order $0 < \alpha < 1$and population sizes that vary across the two groups introduced in [28]. D_t^α denotes the fractional-order derivative operator of order α in system of equations (2.1). As a result, the proposed fractional model involves three population variables for $i = 1,2$: susceptible $S_i(t)$, infected $I_i(t)$, and recovered individuals $R_i(t)$.

$$D_t^\alpha S_1 = \delta_1 - (\xi_{11} I_1 + \xi_{12} I_2 + \gamma_1) S_1,$$

$$D_t^\alpha I_1 = \xi_{11} S_1 I_1 + \xi_{12} S_1 I_2 - (\gamma_1 + \mathcal{V}_1 + P_1) I_1,$$

$$D_t^\alpha R_1 = P_1 I_1 - \gamma_1 R_1,$$

$$D_t^\alpha S_2 = \delta_2 - (\xi_{21} I_1 + \xi_{22} I_2 + \gamma_2) S_2,$$

$$D_t^\alpha I_2 = \xi_{21} S_2 I_1 + \xi_{22} S_2 I_2 - (\gamma_2 + \mathcal{V}_2 + P_2) I_2,$$

$$D_t^\alpha R_2 = P_2 I_2 - \gamma_2 R_2. \tag{2.1}$$

Initial condition

$$S_1(0) = 0.8, I_1(0) = 2, R_1(0) = 1, S_2(0) = 0.8, I_2(0) = 2, R_2(0) = 1, \tag{2.2}$$

For $i = 1,2$, δ_i is the recruitment rate into group i, and γ_i is the natural death rate. The natural recovery rate is ρ_i, and the disease-related death rate is $\mathcal{V}_i$. The transmission rates are ξ_{ii} from S_i to I_i and ξ_{ij} (with $i \neq j$) from S_i to I_j. Without loss of generality, we assume that $\mathcal{V}_i$, P_i, ξ_{ii}, and ξ_{ij} are non-negative constants, and that δ_i and γ_i are positive constants.

To avoid the notation inconsistencies present in the original submission, the natural death rate is now denoted uniformly by Γi (i = 1,2) throughout the manuscript – for the susceptible, infected and recovered sub-populations alike – the recruitment rate by δi, the disease-related death rate by $\mathcal{M}$i, and the recovery rate by Pi; the transmission rates remain ξi j as defined above. These symbols are used consistently in Sections 2, 4 and 5.

3. Basic Definitions

In this section, we will introduce some basic definitions and properties of the theory of fractional calculus that will be later.

Definition 3.1 [30] A real function $f(x), x > 0$ is said to be in the space $C_\mu, \mu \epsilon R$ if there exists a real number $P > \mu$ such that $f(x) = x^p f_1(x)$ where $f_1(x) \epsilon C[0, \infty)$. Clearly $C_\mu < C_\beta$ if $\mu < \beta$.

Definition 3.2 [30] A function $f(x), x > 0$ is said to be in the spaceC_μ^m, $m \epsilon N \cup \{0\}$ if $f^{(m)} \in C_\mu$.

Definition 3.3 [31] The Riemann-Liouville fractional integral operator of the order $\alpha > 0$ of a function, $f \in C_\mu, \mu \geq -1$ is defined as

$$(J_a^\alpha f)(x) = \frac{1}{\Gamma(\alpha)} \int_a^x (x - \tau)^{\alpha - 1} f(\tau) d\tau, x > a, \tag{3.1}$$

$$(J_a^0 f)(x) = f(x). \tag{3.2}$$

All the properties of the operator J^α can be found in [32] which we mention only the following, for $f \in C_\mu, \mu \geq -1, \alpha, \beta \geq 0$, rand $\gamma > -1$ we have

$$\left(J_a^\alpha J_a^\beta f\right)(x) = \left(J_a^{\alpha+\beta} f\right)(x), \tag{3.3}$$

$$\left(J_a^\alpha J_a^\beta f\right)(x) = \left(J_a^\beta J_a^\alpha f\right)(x) \tag{3.4}$$

$$J_a^\alpha x^\gamma = \frac{\Gamma(\gamma+1)}{\Gamma(\alpha+\gamma+1)} x^{\alpha+\gamma}. \tag{3.5}$$

The basic definition of the Riemann–Louville fractional derivative possesses some advantages over other definitions when used to simulate real-world phenomena in the form of a fractional-type differential equation.

Definition 3.4 [33] The fractional derivative of the function $f(x)$ in Caputo's sense is defined as

$$\left(D_a^\alpha f\right)(x) = \left(J_a^{m-\alpha} D^m f\right)(x) = \frac{1}{\Gamma(m-a)} \int_a^x (x-t)^{m-\alpha-1} f^{(m)}(t) dt, \text{ for } m-1 < \alpha < m, m \in N, x > 0. \tag{3.6}$$

Lemma 3.1 If$-1 < \alpha < m$, $m \in$ N and $\mu \geq -1$, then

$$(J_a^\alpha D_a^\alpha f)(x) = f(x) - \sum_{k=0}^{m-1} f^k(a) \left(\frac{(x-a)^k}{k!}\right), a \geq 0 \tag{3.7}$$

$$(D_a^\alpha J_a^\alpha f)(x) = f(x) \tag{3.8}$$

4. Laplace Adomian Decomposition Method

In this section, we will illustrate the basic steps for LADM. We discuss the following important definitions or our research study:

Definition 4.1 [24] A function f on $0 \leq t < \infty$ is exponentially bounded of order $\sigma \in R$ if satisfies $\| f(t) \| \leq Me^{\sigma t}$, for some real constant $M > 0$.

Definition 3.2 The Caputo fractional derivative is defined as follows:

$$\{D^\sigma f(t)\} = s^\sigma L\{f(t)\} - \sum_{k=0}^{m} s^{\sigma-k-1} f^{(k)}(0), \tag{4.a}$$

where $m = \sigma + 1$, and $[\alpha]$ represents the integer part of σ. As a result, the following useful formula is obtained:

$$L(t^\sigma) = \frac{\Gamma(\sigma+1)}{s^{(\sigma+1)}},\ \sigma \in R^+. \tag{4.b}$$

The last-mentioned definitions can be used in this section to discuss the general procedures for solving the proposed mathematical model (2.1). First of all, the Laplace transform is applied to both left-hand and right-hand sides of Eq. (2.1) in the following form:

$$\mathrm{L}(\mathrm{D}_t^\alpha \mathrm{S}_1) = \frac{\delta_1}{s} - \xi_{11}\mathrm{L}(\mathrm{I}_1\mathrm{S}_1) - \xi_{12}\mathrm{L}(\mathrm{I}_2\mathrm{S}_1) - \gamma_1\mathrm{L}(\mathrm{S}_1),$$

$$\mathrm{L}(\mathrm{D}_t^\alpha \mathrm{I}_1) = \xi_{11}\mathrm{L}(\mathrm{S}_1\mathrm{I}_1) + \xi_{12}\mathrm{L}(\mathrm{S}_1\mathrm{I}_2) - \gamma_1\mathrm{L}(\mathrm{I}_1) - \mathcal{V}_1\mathrm{L}(\mathrm{I}_1) - \mathrm{P}_1\mathrm{L}(\mathrm{I}_1),$$

$$\mathrm{L}(\mathrm{D}_t^\alpha \mathrm{R}_1) = \mathrm{P}_1\mathrm{L}(\mathrm{I}_1) - \gamma_1\mathrm{L}(\mathrm{R}_1),$$

$$\mathrm{L}(\mathrm{D}_t^\alpha \mathrm{S}_2) = \frac{\delta_2}{s} - \xi_{21}\mathrm{L}(\mathrm{I}_1\mathrm{S}_2) - \xi_{22}\mathrm{L}(\mathrm{I}_2\mathrm{S}_2) - \gamma_2\mathrm{L}(\mathrm{S}_2),$$

$$\mathrm{L}(\mathrm{D}_t^\alpha \mathrm{I}_2) = \xi_{21}\mathrm{L}(\mathrm{S}_2\mathrm{I}_1) + \xi_{22}\mathrm{L}(\mathrm{S}_2\mathrm{I}_2) - \gamma_2\mathrm{L}(\mathrm{I}_2) - \mathcal{V}_2\mathrm{L}(\mathrm{I}_2) - \mathrm{P}_2\mathrm{L}(\mathrm{I}_2),$$

$$L(D_t^\alpha R_2) = P_2 L(\mathrm{I}_2) - \gamma_2 L(R_2). \tag{4.1}$$

Then, by applying the formula (4.a) to Eq. (4.1), we get

$$S^{\alpha}L(S_1) - S^{\alpha-1}S_1(0) = \frac{\delta_1}{S} - \xi_{11}L(I_1S_1) - \xi_{12}L(I_2S_1) - \gamma_1 L(S_1),$$

$$S^{\alpha}L(I_1) - S^{\alpha-1}I_1(0) = \xi_{11}L(S_1I_1) + \xi_{12}L(S_1I_2) - \gamma_1 L(I_1) - \mathcal{V}_1 L(I_1) - P_1L(I_1),$$

$$S^{\alpha}L(R_1) - S^{\alpha-1}R_1(0) = P_1L(I_1) - \gamma_1 L(R_1),$$

$$S^{\alpha}L(S_2) - S^{\alpha-1}S_2(0) = \frac{\delta_2}{s} - \xi_{21}L(I_1S_2) - \xi_{22}L(I_2S_2) - \gamma_2 L(S_2),$$

$$S^{\alpha}L(I_2) - S^{\alpha-1}I_2(0) = \xi_{21}L(S_2I_1) + \xi_{22}L(S_2I_2) - \gamma_2 L(I_2) - \mathcal{V}_2 L(I_2) - P_2L(I_2),$$

$$S^{\alpha}L(R_2) - S^{\alpha-1}R_2(0) = P_2L(I_2) - \gamma_2 L(R_2). \tag{4.2}$$

Next, by substituting the initial conditions in Eq. (2.2) into the model (4.2), we get

$$L(S_1) = \frac{S_1(0)}{S} + \frac{\delta_1}{S^{\alpha+1}} - \frac{\xi_{11}}{S^{\alpha}}L(I_1S_1) - \frac{\xi_{12}}{S^{\alpha}}L(I_2S_1) - \frac{\gamma_1}{S^{\alpha}}L(S_1),$$

$$L(I_1) = \frac{I_1(0)}{S} + \frac{\xi_{11}}{S^{\alpha}}L(S_1I_1) + \frac{\xi_{12}}{S^{\alpha}}L(S_1I_2) - \frac{\gamma_1}{S^{\alpha}}L(I_1) - \frac{\mathcal{V}_1}{S^{\alpha}}L(I_1) - \frac{P_1}{S^{\alpha}}L(I_1),$$

$$L(R_1) = \frac{R_1(0)}{S} + \frac{P_1}{S^{\alpha}}L(I_1) - \frac{\gamma_1}{S^{\alpha}}L(R_1),$$

$$L(S_2) = \frac{S_2(0)}{S} + \frac{\delta_2}{S^{\alpha+1}} - \frac{\xi_{21}}{S^{\alpha}}L(I_1S_2) - \frac{\xi_{22}}{S^{\alpha}}L(I_2S_2) - \frac{\gamma_2}{S^{\alpha}}L(S_2),$$

$$L(I_2) = \frac{I_2(0)}{S} + \frac{\xi_{21}}{S^{\alpha}}L(S_2I_1) + \frac{\xi_{22}}{S^{\alpha}}L(S_2I_2) - \frac{\gamma_2}{S^{\alpha}}L(I_2) - \frac{\mathcal{V}_2}{S^{\alpha}}L(I_2) - \frac{P_2}{S^{\alpha}}L(I_2),$$

$$L(R_2) = \frac{R_2(0)}{S} + \frac{P_2}{S^{\alpha}}L(I_2) - \frac{\gamma_2}{S^{\alpha}}L(R_2). \tag{4.3}$$

The proposed method gives the solution as an infinite series. Let the value of $A = I_1S_1, B = I_2S_1, C = I_2S_2$ and $E = S_2I_1$to be able to apply the Adomian decomposition method. We consider the solution as an infinite series in the form

$$S_1 = \sum_{n=0}^{\infty} S_{1n},\ I_{12} = \sum_{n=0}^{\infty} I_{1n},\ R_{12} = \sum_{n=0}^{\infty} R_{1n},\ S_{22} = \sum_{n=0}^{\infty} S_{2n},$$

$$I_{22} = \sum_{n=0}^{\infty} I_{2n},\ R_{2n} = \sum_{n=0}^{\infty} R_{2n}, \tag{4.4}$$

Then, by decomposing the nonlinear part named A, B, C and E in the following form

$$A = \sum_{n=0}^{\infty} A_n,\ B = \sum_{n=0}^{\infty} B_n,\ C = \sum_{n=0}^{\infty} C_n,\ E = \sum_{n=0}^{\infty} E_n, \tag{4.5}$$

Here, A_n, B_n, C_n and E_n can be computed using the convolution operation as

$$A_n = \frac{1}{\Gamma(n+1)}\frac{d^n}{d\eta^n}\left[\sum_{i=0}^{n}\eta^i I_i \sum_{i=0}^{n}\eta^i S_{1,i}\right]_{\eta=0},\ B_n = \frac{1}{\Gamma(n+1)}\frac{d^n}{d\eta^n}\left[\sum_{i=0}^{n}\eta^i I_i \sum_{i=0}^{n}\eta^i R_i\right]_{\eta=0},$$

$$C_n = \frac{1}{\Gamma(n+1)}\frac{d^n}{d\eta^n}\left[\sum_{i=0}^{n}\eta^i R_i \sum_{i=0}^{n}\eta^i S_{1,i}\right]_{\eta=0},\ E_n = \frac{1}{\Gamma(n+1)}\frac{d^n}{d\eta^n}\left[\sum_{i=0}^{n}\eta^i I_i \sum_{i=0}^{n}\eta^i S_{2,i}\right]_{\eta=0}, \tag{4.6}$$

By substituting Eq. (4.4- 4.6) into Eq. (4.3) and by matching the two sides of the equation yields the following iterative algorithm we have resulted in the form.

$$L\left(\sum_{n=0}^{\infty} S_{1n}\right) = \frac{S_{10}}{S} + \frac{\delta_1}{S^{\alpha+1}} - \frac{\xi_{21}}{S^{\alpha}} L\left(\sum_{n=0}^{\infty} A_n\right) - \frac{\xi_{12}}{S^{\alpha}} L\left(\sum_{n=0}^{\infty} B_n\right) - \frac{\gamma_1}{S^{\alpha}} L\left(\sum_{n=0}^{\infty} S_{1n}\right),$$

$$L\left(\sum_{n=0}^{\infty} I_{1n}\right) = \frac{I_{10}}{S} + \frac{\xi_{11}}{S^{\alpha}} L\left(\sum_{n=0}^{\infty} A_n\right) + \frac{\xi_{12}}{S^{\alpha}} L\left(\sum_{n=0}^{\infty} B_n\right) - \frac{\gamma_1}{S^{\alpha}} L\left(\sum_{n=0}^{\infty} I_{1n}\right) - \frac{\mathcal{V}_1}{S^{\alpha}} L\left(\sum_{n=0}^{\infty} I_{1n}\right) - \frac{P_1}{S^{\alpha}} L\left(\sum_{n=0}^{\infty} I_{1n}\right),$$

$$L\left(\sum_{n=0}^{\infty} R_{1n}\right) = \frac{R_{10}}{S} + \frac{P_1}{S^{\alpha}} L\left(\sum_{n=0}^{\infty} I_{1n}\right) - \frac{\gamma_1}{S^{\alpha}} L\left(\sum_{n=0}^{\infty} R_{1n}\right),$$

$$L\left(\sum_{n=0}^{\infty} S_{2n}\right) = \frac{S_{20}}{S} + \frac{\delta_2}{S^{\alpha+1}} - \frac{\xi_{21}}{S^{\alpha}} L\left(\sum_{n=0}^{\infty} E_n\right) - \frac{\xi_{22}}{S^{\alpha}} L\left(\sum_{n=0}^{\infty} C_n\right) - \frac{\gamma_2}{S^{\alpha}} L\left(\sum_{n=0}^{\infty} S_{2n}\right),$$

$$L\left(\sum_{n=0}^{\infty} I_{2n}\right) = \frac{I_{20}}{S} + \frac{\xi_{21}}{S^{\alpha}} L\left(\sum_{n=0}^{\infty} E_n\right) + \frac{\xi_{12}}{S^{\alpha}} L\left(\sum_{n=0}^{\infty} B_n\right) + \frac{\xi_{22}}{S^{\alpha}} L\left(\sum_{n=0}^{\infty} C_n\right)$$

$$-\frac{\gamma_2}{S^{\alpha}} L\left(\sum_{n=0}^{\infty} I_{2n}\right) - \frac{\mathcal{V}_2}{S^{\alpha}} L\left(\sum_{n=0}^{\infty} I_{2n}\right) - \frac{P_2}{S^{\alpha}} L\left(\sum_{n=0}^{\infty} I_{2n}\right),$$

$$L\left(\sum_{n=0}^{\infty} R_{2n}\right) = \frac{R_{20}}{S} + \frac{P_2}{S^{\alpha}} L\left(\sum_{n=0}^{\infty} I_{2n}\right) - \frac{\gamma_2}{S^{\alpha}} L\left(\sum_{n=0}^{\infty} R_{2n}\right). \tag{4.7}$$

By equating both sides of Equation (4.7), we obtain the following iterative algorithm:

$L(S_{10}) = \frac{S_{10}}{S}$, $\quad L(I_{10}) = \frac{I_{10}}{S}$, $\quad L(R_{10}) = \frac{R_{10}}{S}$,

$L(S_{20}) = \frac{S_{20}}{S}$, $\quad L(I_{20}) = \frac{I_{20}}{S}$, $\quad L(R_{20}) = \frac{R_{20}}{S}$,

$L(S_{11}) = \frac{\delta_1}{S^{\alpha+1}} - \frac{\xi_{11}}{S^{\alpha}} L(A_0) - \frac{\xi_{12}}{S^{\alpha}} L(B_0) - \frac{\gamma_1}{S^{\alpha}} L(S_{10})$,

$L(I_{11}) = \frac{\xi_{11}}{S^{\alpha}} L(A_0) + \frac{\xi_{12}}{S^{\alpha}} L(B_0) - \frac{\gamma_1}{S^{\alpha}} L(I_{10}) - \frac{\mathcal{V}_1}{S^{\alpha}} L(I_{10}) - \frac{P_1}{S^{\alpha}} L(I_{10})$,

$L(R_{11}) = \frac{P_1}{S^{\alpha}} L(I_{10}) - \frac{\gamma_1}{S^{\alpha}} L(R_{10})$,

$L(S_{21}) = \frac{\delta_2}{S^{\alpha+1}} - \frac{\xi_{21}}{S^{\alpha}} L(E_0) - \frac{\xi_{22}}{S^{\alpha}} L(C_0) - \frac{\gamma_2}{S^{\alpha}} L(S_{20})$,

$L(I_{21}) = \frac{\xi_{21}}{S^{\alpha}} L(E_0) + \frac{\xi_{22}}{S^{\alpha}} L(C_0) - \frac{\gamma_2}{S^{\alpha}} L(I_{20}) - \frac{\mathcal{V}_2}{S^{\alpha}} L(I_{20}) - \frac{P_2}{S^{\alpha}} L(I_{20})$,

$L(R_{21}) = \frac{P_2}{S^{\alpha}} L(I_{20}) - \frac{\gamma_2}{S^{\alpha}} L(R_{20}), \dots,$

$L(S_{1n}) = -\frac{\xi_{11}}{S^{\alpha}} L(A_{n-1}) - \frac{\xi_{12}}{S^{\alpha}} L(B_{n-1}) - \frac{\gamma_1}{S^{\alpha}} L(S_{1n-1})$,

$L(I_{1n}) = \frac{\xi_{11}}{S^{\alpha}} L(A_{n-1}) + \frac{\xi_{12}}{S^{\alpha}} L(B_{n-1}) - \frac{\gamma_1}{S^{\alpha}} L(I_{1n-1}) - \frac{\mathcal{V}_1}{S^{\alpha}} L(I_{1n-1}) - \frac{P_1}{S^{\alpha}} L(I_{1n-1})$,

$L(R_{1n}) = \frac{P_1}{S^{\alpha}} L(I_{1n-1}) - \frac{\gamma_1}{S^{\alpha}} L(R_{1n-1})$,

$L(S_{2n}) = -\frac{\xi_{21}}{S^{\alpha}} L(E_{n-1}) - \frac{\xi_{22}}{S^{\alpha}} L(C_{n-1}) - \frac{\gamma_2}{S^{\alpha}} L(S_{2n-1})$,

$L(I_{2n}) = \frac{\xi_{21}}{S^{\alpha}} L(E_{n-1}) + \frac{\xi_{22}}{S^{\alpha}} L(C_{n-1}) - \frac{\gamma_2}{S^{\alpha}} L(I_{2n-1}) - \frac{\mathcal{V}_2}{S^{\alpha}} L(I_{2n-1}) - \frac{P_2}{S^{\alpha}} L(I_{2n-1})$,

$$L(R_{2n}) = \frac{P_2}{S^{\alpha}} L(I_{2n-1}) - \frac{\gamma_2}{S^{\alpha}} L(R_{2n-1}). \tag{4.8}$$

Finally, by taking the inverse transform of Eq. (4.8), we have the following equation

$S_{10} = S_{100}, I_{10} = I_{100}, \; R_{10} = R_{100},$

$S_{20} = S_{200}, I_{20} = I_{200}, R_{20} = R_{200},$

$S_{11} = [\delta_1 - \xi_{11}A_0 - \xi_{12}B_0 - \gamma_1 S_{100}]\frac{t^{\alpha}}{\Gamma(\alpha+1)},$

$I_{11} = [\xi_{11}A_0 + \xi_{12}B_0 - \gamma_1 I_{100} - \mathcal{V}_1 I_{100} - P_1 I_{100}]\frac{t^{\alpha}}{\Gamma(\alpha+1)},$

$R_{11} = [P_1 I_{100} - \gamma_1 R_{100}]\frac{t^{\alpha}}{\Gamma(\alpha+1)},$

$S_{21} = [-\xi_{21}E_0 - \xi_{22}C_0 - \gamma_2 S_{200}]\frac{t^{\alpha}}{\Gamma(\alpha+1)},$

$I_{21} = [\xi_{21}E_0 + \xi_{22}C_0 - \gamma_2 I_{200} - \mathcal{V}_2 I_{100} - P_2 I_{200}]\frac{t^{\alpha}}{\Gamma(\alpha+1)},$

$$R_{21} = [P_2 I_{200} - \gamma_2 R_{200}]\frac{t^{\alpha}}{\Gamma(\alpha+1)}, \tag{4.9}$$

Similarly, at the final step, we get the rest of the terms as infinite series as,

$S_1(t) = \sum_{i=0}^{\infty} S_{1i}, I_1(t) = \sum_{i=0}^{\infty} I_{1i}, R_1(t) = \sum_{i=0}^{\infty} R_{2i},$

$$S_2(t) = \sum_{i=0}^{\infty} S_{2i}, I_2(t) = \sum_{i=0}^{\infty} I_{2i}, R_2(t) = \sum_{i=0}^{\infty} R_{2i}. \tag{4.10}$$

Equation (4.10) solves the main SIR model of Eq. (2.1) which will be illustrated in the next section.

5. Numerical Simulations

In this section, we test the effectiveness of the proposed technique by examining the acquired results for model (2.1) for different α. The numerical simulations are presented by taking partial parameters from numerical simulations in [29]. In this section, the values of various parameters are presented for two different cases (Table **1**-**2**) .

The results obtained by LADM closely match the numerical (ODE45) solutions when $\alpha = 1$. In this study, two cases are examined to evaluate the model performance for $\alpha = 1, \alpha = 0.75$, and $\alpha = 0.5$. Fig. (**1**–**36**) presents a comparison between the results obtained using LADM and those generated by MATLAB's ODE45 (Runge–Kutta 4th order method) across various model categories. It is evident from this figure that the proposed technique is efficient and accurate, as it perfectly agrees with the MATLAB code results.

The choice of $\alpha = 0.75$ and $\alpha = 0.5$, in addition to the classical case $\alpha = 1$, is intended to illustrate how progressively stronger memory effects influence the epidemic process: smaller values of α place increasing weight on the past history of the susceptible, infected and recovered sub-populations, which in the present model is reflected in a slower, more gradual approach toward the equilibrium levels and a broadened infection peak, consistent with the interpretation of α as a memory (hereditary) parameter of the disease-transmission process rather than a purely mathematical tuning constant. It should also be stressed that ODE45 solves only integer-order ($\alpha = 1$) systems and cannot be applied directly when $\alpha \neq 1$; for $\alpha = 0.75$ and $\alpha = 0.5$ no independent numerical solver is therefore available for comparison. The accuracy of the LADM solution for $\alpha \neq 1$ is instead inferred indirectly, from (i) the close agreement between LADM and ODE45 already demonstrated for the integer-order case $\alpha = 1$, and (ii) the rapidly decaying magnitude of successive terms in the LADM series, which confirms the fast convergence of the approximation for all values of α considered.

Table 1: Parameter descriptions of the SIR nonlinear system.

Case A	$\delta_1 = 0.3; \delta_2 = 0.2, \mathcal{V}_1 = 0.4, \mathcal{V}_2 = 0.4, \mathrm{P}_1 = 0.2, \mathrm{P}_2 = 0.3,$ $\xi_{11}(1) = 0.6, \xi_{11}(2) = 0.7, \xi_{21}(1) = 0.1, \xi_{21}(2) = 0.6,$ $\gamma_1 = 0.3, \xi_{12}(1) = 0.2, \xi_{12}(2) = 0.5, \xi_{22}(1) = 0.7, \xi_{22}(2) = 0.8,$ $\gamma_2 = 0.2,$

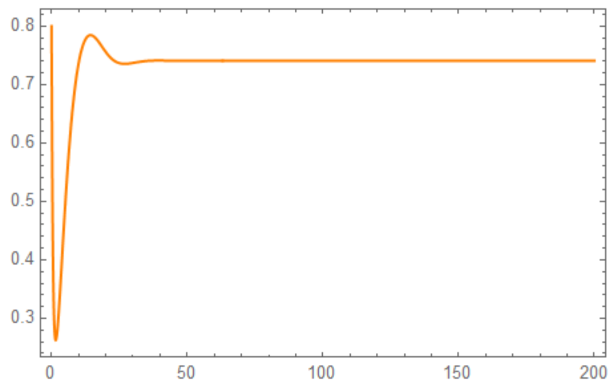

Figure 1: The numerical solution of $S_1(t)$(ODE45) for $\alpha = 1$.

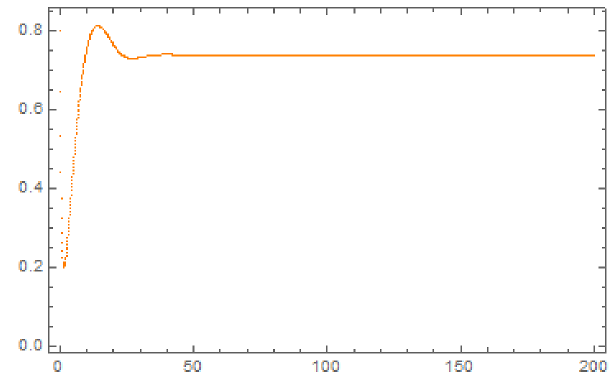

Figure 2: The approximate solution of $S_1(t)$(LADM) for $\alpha = 1$.

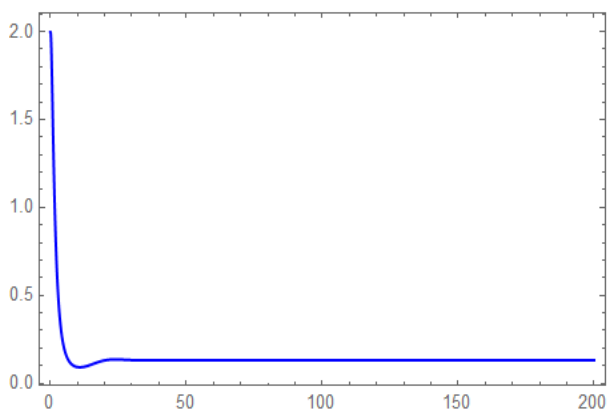

Figure 3: The numerical solution of $I_1(t)$(ODE45) for $\alpha = 1$.

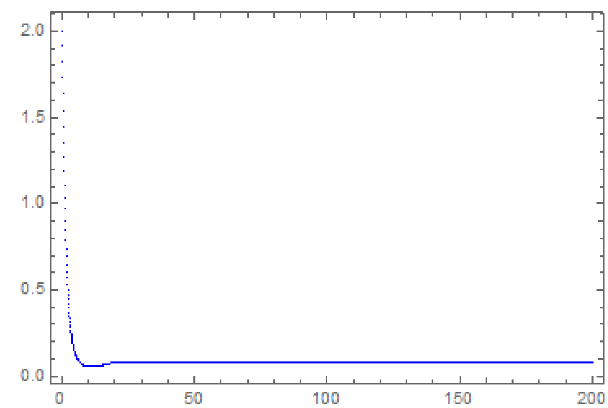

Figure 4: The approximate solution of $I_1(t)$(LADM) for $\alpha = 1$.

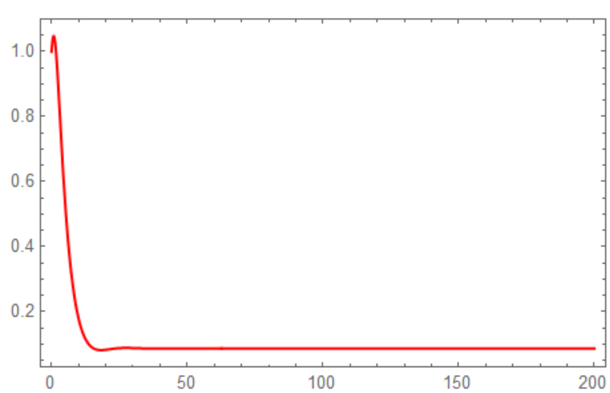

Figure 5: The numerical solution of $R_1(t)$(ODE45) for $\alpha = 1$.

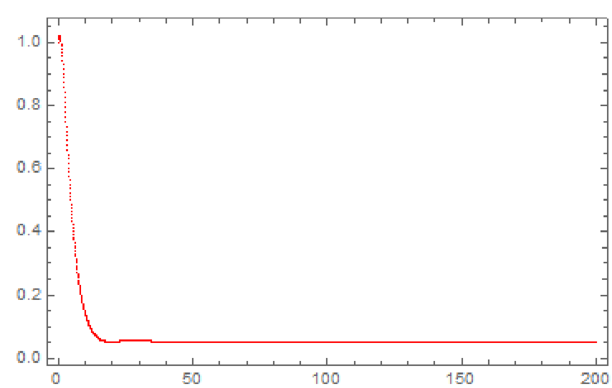

Figure 6: The approximate solution of $R_1(t)$(LADM) for $\alpha = 1$.

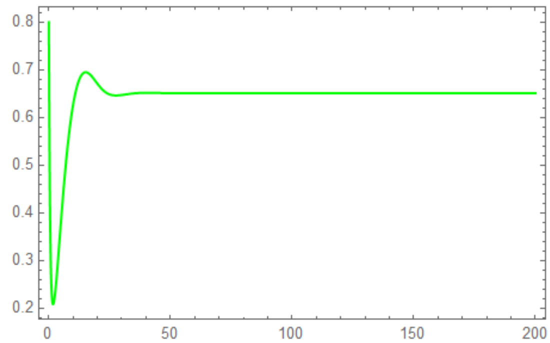

Figure 7: The numerical solution of $S_2(t)$(ODE45) for $\alpha = 1$.

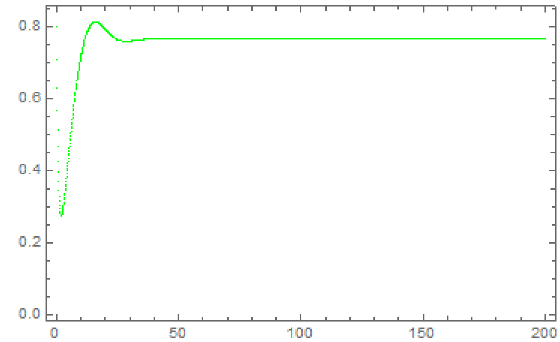

Figure 8: The approximate solution of $S_2(t)$(LADM) for $\alpha = 1$.

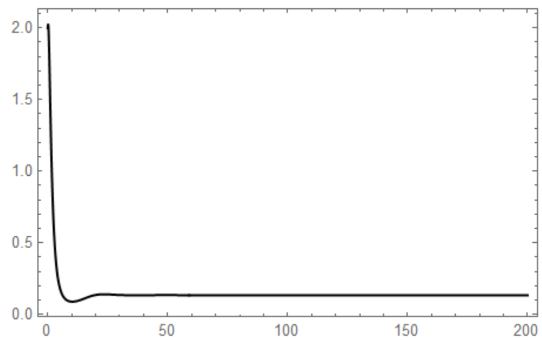

Figure 9: The numerical solution of $I_2(t)$(ODE45) for $\alpha = 1$.

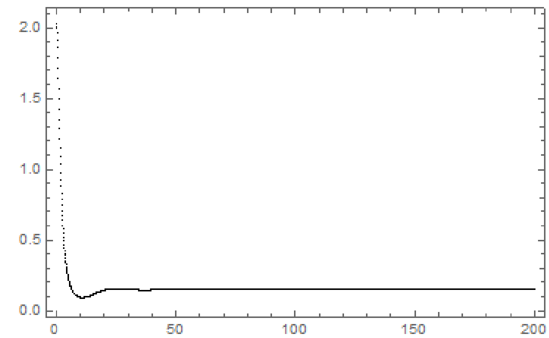

Figure 10: The approximate solution of $I_2(t)$(LADM) for $\alpha = 1$.

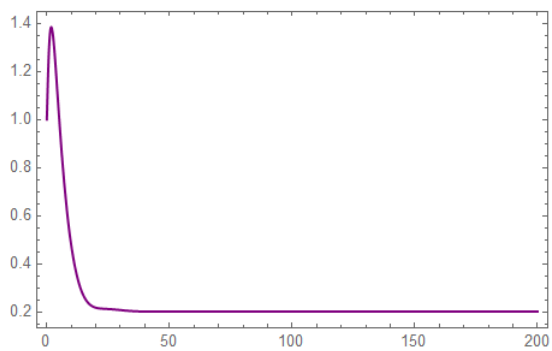

Figure 11: The numerical solution of $R_2(t)$(ODE45) for $\alpha = 1$.

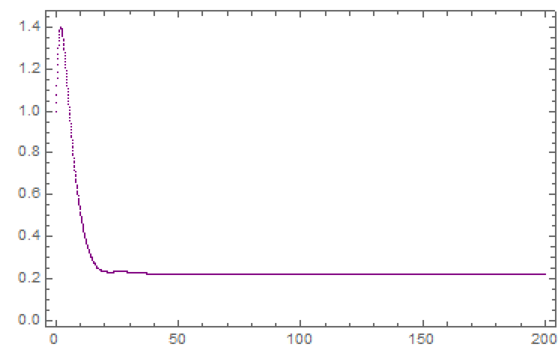

Figure 12: The approximate solution of $R_2(t)$(LADM) for $\alpha = 1$.

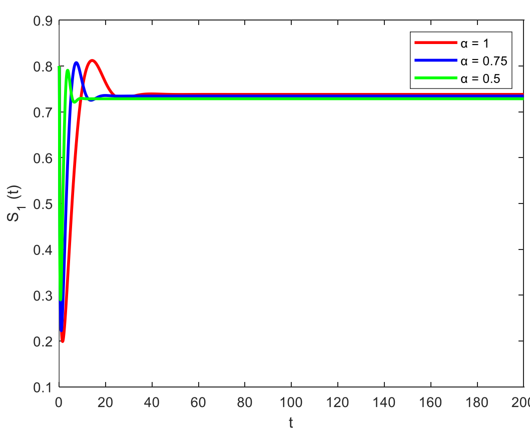

Figure 13: The solution of $S_1(t)$ obtained by LADM for different values of α, (a) of $\alpha = 1$, (b) of $\alpha = 0.75$, (c) of $\alpha = 0.5$ and $0 \le t \le 200$.

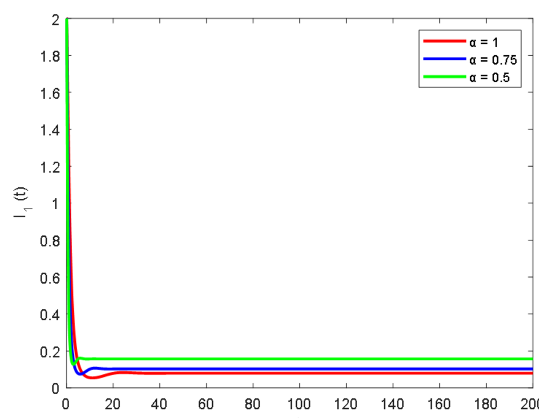

Figure 14: The solution of $I_1(t)$ obtained by LADM for different values of α, (a) of $\alpha = 1$, (b) of $\alpha = 0.75$, (c) of $\alpha = 0.5$ and $0 \le t \le 200$.

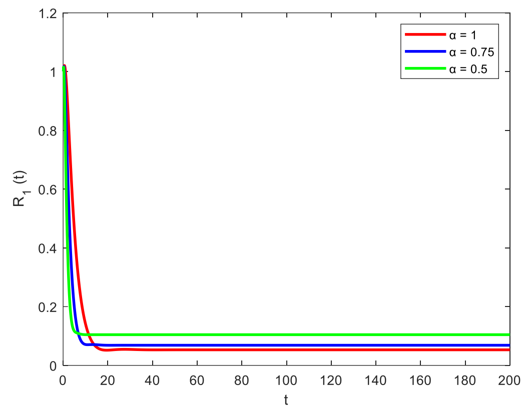

Figure 15: The solution of $R_1(t)$ obtained by LADM for different values of α, (a) of $\alpha = 1$, (b) of $\alpha = 0.75$, (c) of $\alpha = 0.5$ and $0 \le t \le 200$.

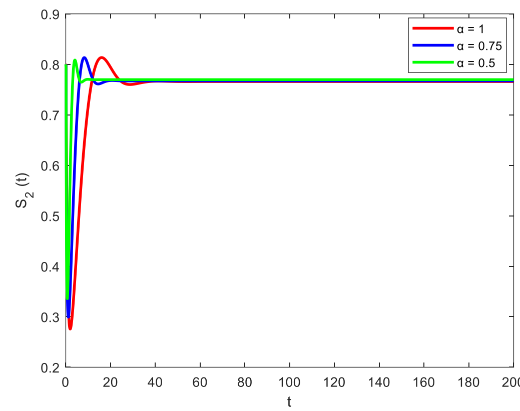

Figure 16: The solution of $S_2(t)$ obtained by LADM for different values of α, (a) of $\alpha = 1$, (b) of $\alpha = 0.75$, (c) of $\alpha = 0.5$ and $0 \le t \le 200$.

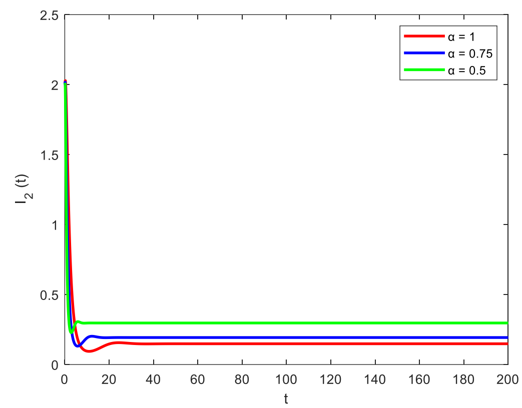

Figure 17: The solution of $I_2(t)$ obtained by LADM for different values of α, (a) of $\alpha = 1$, (b) of $\alpha = 0.75$, (c) of $\alpha = 0.5$ and $0 \le t \le 200$.

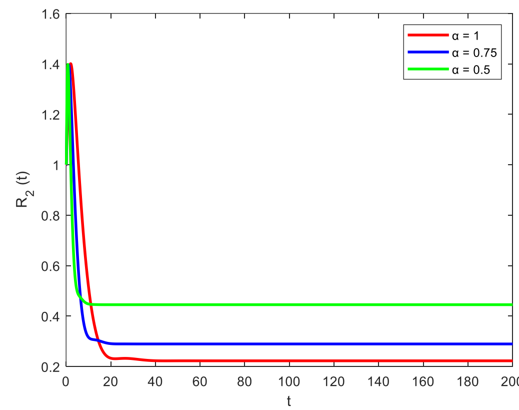

Figure 18: The solution of $R_2(t)$ obtained by LADM for different values of α, (a) of $\alpha = 1$, (b) of $\alpha = 0.75$, (c) of $\alpha = 0.5$ and $0 \le t \le 200$.

Table 2: Parameter descriptions of the SIR nonlinear system.

Case B	$\delta 1 = 0.6, \delta 2 = 0.5, P1 = 0.2, P2 = 0.1, \nu 1 = 0.1, \nu 2 = 0.4,$ $\xi_{11}(1) = 0.6, \xi_{11}(2) = 0.7, \xi_{21}(1) = 0.1, \xi_{21}(2) = 0.6,$ $\gamma_1 = 0.3, \xi_{12}(1) = 0.2, \xi_{12}(2) = 0.5, \xi_{22}(1) = 0.7, \xi_{22}(2) = 0.8,$ $\gamma_2 = 0.2$.

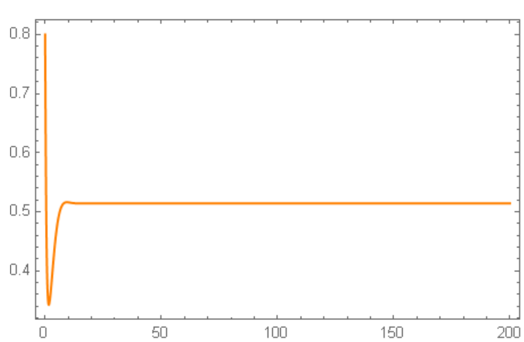

Figure 19: The numerical solution of $S_1(t)$(ODE45) for $\alpha = 1$.

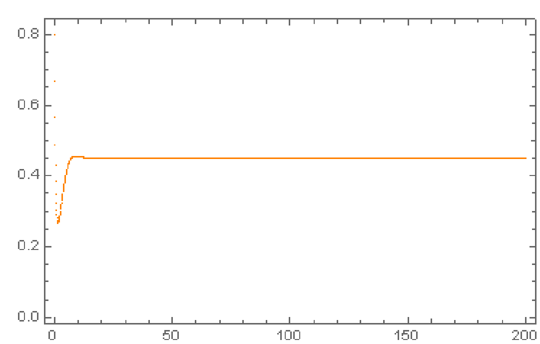

Figure 20: The approximate solution of $S_1(t)$(LADM) for $\alpha = 1$.

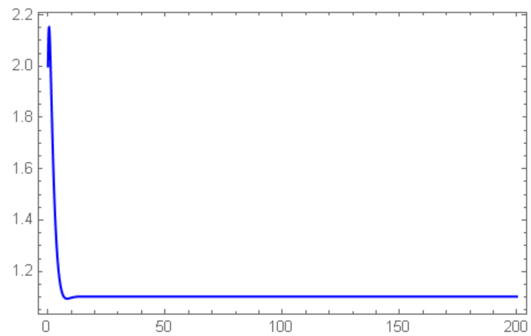

Figure 21: The numerical solution of $I_1(t)$(ODE45) for $\alpha = 1$.

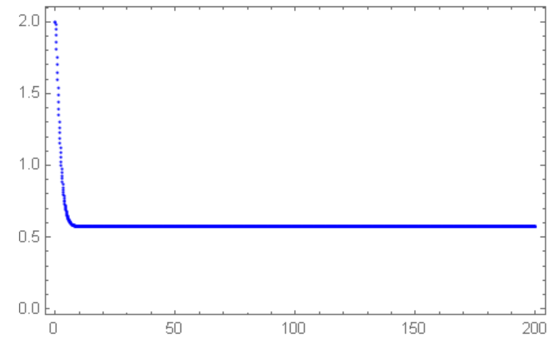

Figure 22: The approximate solution of $I_1(t)$(LADM) for $\alpha = 1$.

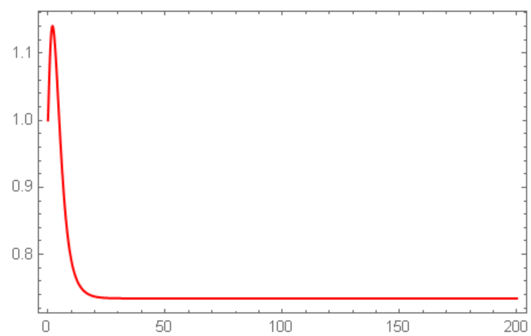

Figure 23: The numerical solution of $R_1(t)$(ODE45) for $\alpha = 1$.

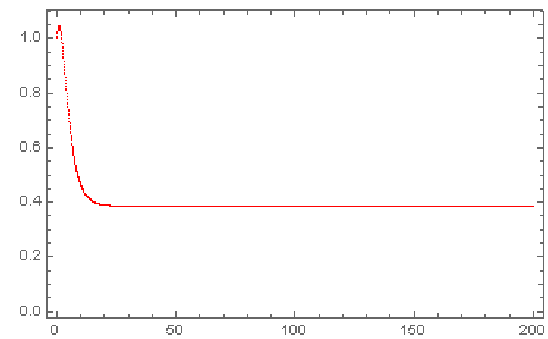

Figure 24: The approximate solution of $R_1(t)$(LADM) for $\alpha = 1$.

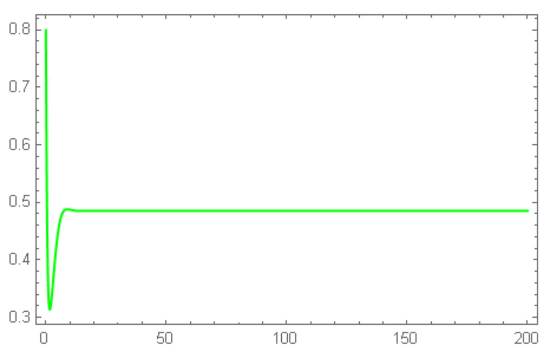

Figure 25: The numerical solution of $S_2(t)$(ODE45) for $\alpha = 1$.

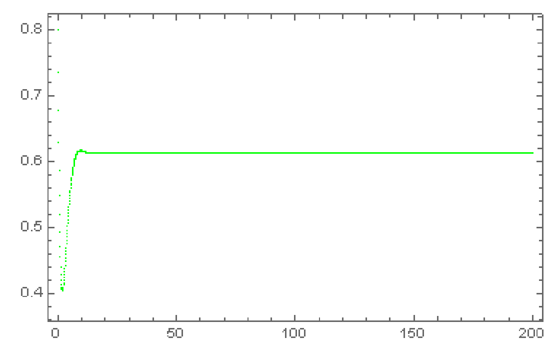

Figure 26: The approximate solution of $S_2(t)$(LADM) for $\alpha = 1$.

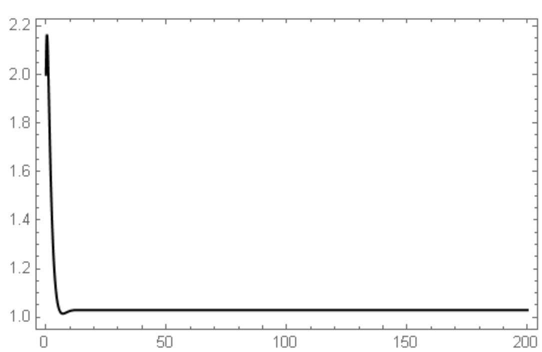

Figure 27: The numerical solution of $I_2(t)$(ODE45) for $\alpha = 1$.

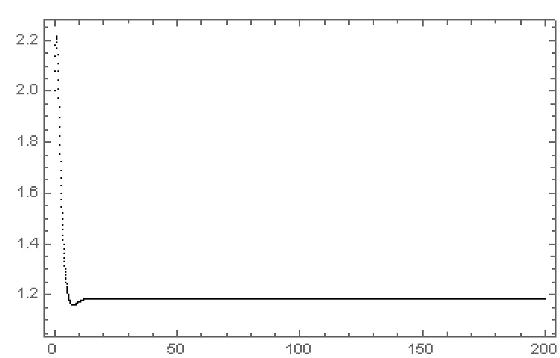

Figure 28: The approximate solution of $I_2(t)$(LADM) for $\alpha = 1$.

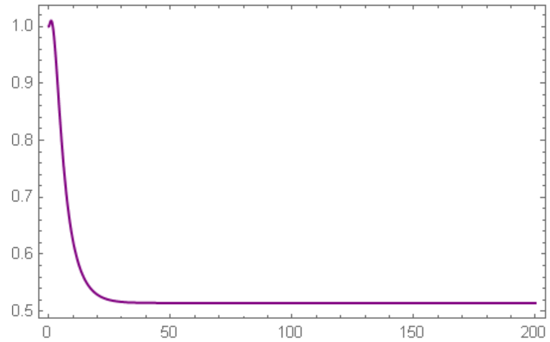

Figure 29: The numerical solution of $R_2(t)$(ODE45) for $\alpha = 1$.

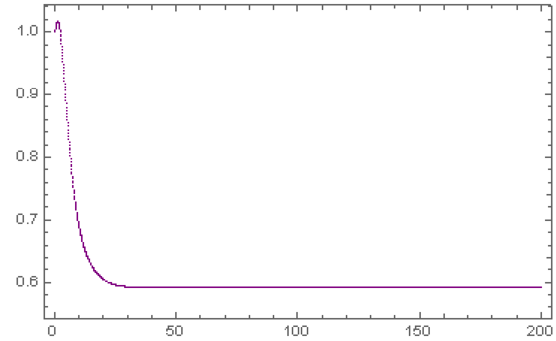

Figure 30: The approximate solution of $R_2(t)$(LADM) for $\alpha = 1$.

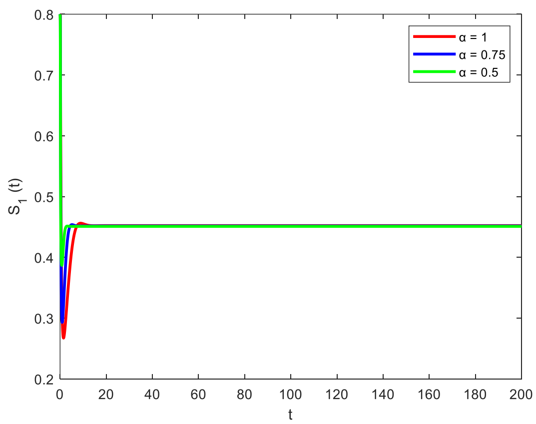

Figure 31: The solution of $S_1(t)$ obtained by LADM for different values of α, (a) of $\alpha = 1$, (b) of $\alpha = 0.75$, (c) of $\alpha = 0.5$ and $0 \le t \le 200$.

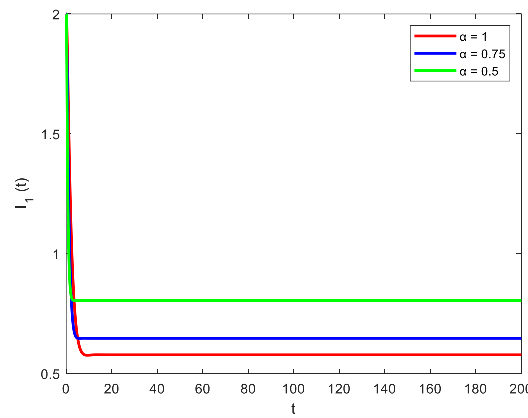

Figure 32: The solution of $I_1(t)$ obtained by LADM for different values of α, (a) of $\alpha = 1$, (b) of $\alpha = 0.75$, (c) of $\alpha = 0.5$ and $0 \le t \le 200$.

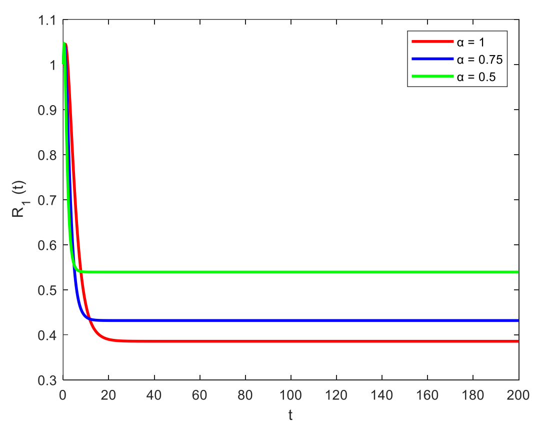

Figure 33: The solution of $R_1(t)$ obtained by LADM for different values of α, (a) of $\alpha = 1$, (b) of $\alpha = 0.75$, (c) of $\alpha = 0.5$ and $0 \le t \le 200$.

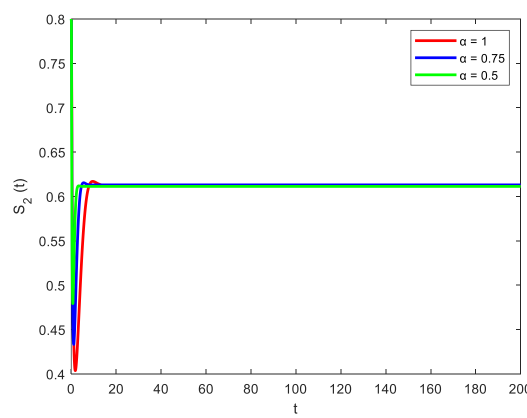

Figure 34: The solution of $S_2(t)$ obtained by LADM for different values of α, (a) of $\alpha = 1$, (b) of $\alpha = 0.75$, (c) of $\alpha = 0.5$ and $0 \le t \le 200$.

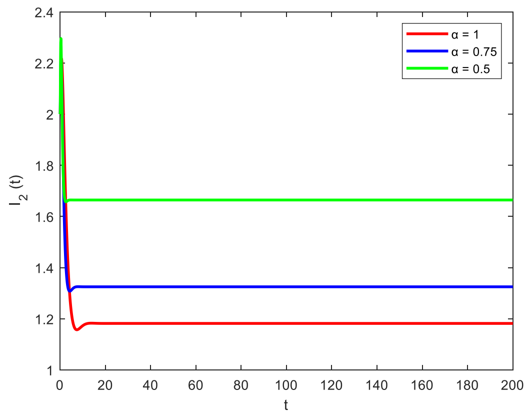

Figure 35: The solution of $I_2(t)$ obtained by LADM for different values of α, (a) of $\alpha = 1$, (b) of $\alpha = 0.75$, (c) of $\alpha = 0.5$ and $0 \leq t \leq 200$.

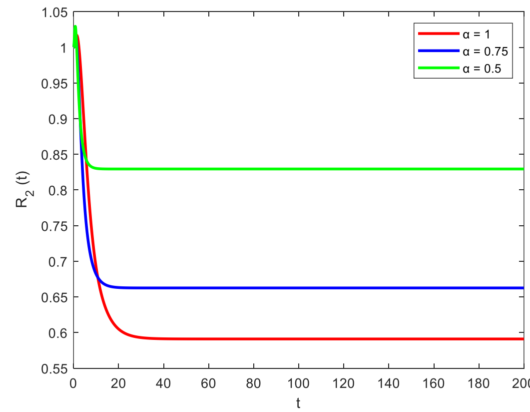

Figure 36: The solution of $R_2(t)$ obtained by LADM for different values of α, (a) of $\alpha = 1$, (b) of $\alpha = 0.75$, (c) of $\alpha = 0.5$ and $0 \leq t \leq 200$.

6. Conclusions

This research developed a nonlinear SIR model utilizing a modified Caputo fractional derivative to examine the transmission dynamics of infectious diseases. The model was effectively resolved employing two distinct methodologies: the fourth-order Runge–Kutta method and the Laplace–Adomian decomposition method. The results obtained yield precise solutions and are examined for varying values of the fractional-order parameter α and diverse transmission rates. All results have been examined and contrasted across various cases. The results show that all values of α and transmission rates are very accurate and stable. Our results and methodologies can be further expanded or generalized to address additional intriguing nonlinear models that emerge from diverse phenomena in physics and engineering. The results are also applicable to models developed with alternative fractional derivatives.

Comparing the three fractional orders considered, α = 1, α = 0.75 and α = 0.5, the simulations show that as α decreases the infected sub-populations I1 and I2 reach their peak later and at a lower amplitude, while the susceptible and recovered compartments approach their long-run levels more gradually; in other words, the memory effect captured by the fractional derivative tends to flatten and delay the epidemic curve relative to the classical integer-order case. This suggests that populations whose transmission or recovery process carries a stronger hereditary component may experience a slower-burning, less sharply peaked outbreak, a biologically relevant insight that the classical integer-order SIR model cannot provide. The present study nevertheless has some limitations: the model assumes a constant total population with no age-structure, it does not include vaccination or time-dependent transmission and recovery rates, and the LADM solution is presented as a truncated series whose accuracy for α ≠ 1 could not be benchmarked against an independent fractional-order solver. Future work will extend the model to include vaccination strategies, age-structured or spatially distributed populations, and time-varying parameters, and will compare the LADM series against dedicated fractional numerical schemes (e.g. the Adams–Bashforth–Moulton predictor-corrector method) for α ≠ 1.

Conflict of Interest

The authors declare that they have no conflict of interest.

Funding

This research received no external funding.

References

[1] Hassouna M, Ouhadan A, El Kinani EH. On the solution of fractional order SIS epidemic model. Chaos Solitons Fractals. 2018; 117: 168-74. https://doi.org/10.1016/j.chaos.2018.10.023

[2] Algolam MS, Almalahi M, Aldwoah K, Awaad AS, Suhail M, Alshammari FA, *et al*. Theoretical and numerical analysis of the SIR model and its symmetric cases with power Caputo fractional derivative. Fractal Fract. 2025; 9(4): 251. https://doi.org/10.3390/fractalfract9040251

[3] Liu A, Yasin F, Afzal Z, Nazeer W. Analytical solution of a non-linear fractional order SIS epidemic model utilizing a new technique. Results Phys. 2023; 73: 123-9. https://doi.org/10.1016/j.aej.2023.04.018

[4] Kim J. Influence of fractional order on the behavior of a normalized time-fractional SIR model. Mathematics. 2024; 12: 456. https://doi.org/10.3390/math12193081

[5] Mouaouine A, Boukhouima A, Hattaf K, Yousfi N. A fractional order SIR epidemic model with nonlinear incidence rate. Adv Differ Equ. 2018; 2018: 160. https://doi.org/10.1186/s13662-018-1613-z

[6] Yavuz M, Özdemir N. Analysis of an epidemic spreading model with exponential decay law. Math Methods Appl Sci. 2020; 43: 1247-55. https://doi.org/10.36753/mathenot.691638

[7] Sene N. SIR epidemic model with Mittag-Leffler fractional derivative. Chaos Solitons Fractals. 2020; 137: 109833. https://doi.org/10.1016/j.chaos.2020.109833

[8] Taghvaei A, Georgiou TT, Norton L, Tannenbaum A. Fractional SIR epidemiological models. Sci Rep. 2020; 10: 20882. https://doi.org/10.1038/s41598-020-77849-7

[9] Alqahtani RT. Mathematical model of SIR epidemic system (COVID-19) with fractional derivative. Adv Differ Equ. 2021; 2021: Article number 2. https://doi.org/10.1186/s13662-020-03192-w

[10] Mousa MM, Alsharari F. A comparative numerical study for a fractional-order SIR model. Mathematics. 2021; 9(22): 2847. https://doi.org/10.3390/math9222847

[11] Qazza A, Saadeh R. On the analytical solution of fractional SIR epidemic model. arXiv. 2023. https://doi.org/10.1155/2023/6973734

[12] Alazman I, Mishra MN, Alkahtani BS, Dubey RS. Analysis of infection and diffusion coefficient in an SIR model. Fractal Fract. 2024; 8(9): 537. https://doi.org/10.3390/fractalfract8090537

[13] Prodanov D. Exponential series approximation of the SIR epidemiological model. Front Phys. 2024; 12: 1469663. https://doi.org/10.3389/fphy.2024.1469663

[14] Murph AC, Gibson GC, Beesley LJ, Panda N, Castro LA, Del Valle SY. Mapping incidence and prevalence peak data for SIR modeling applications. J Math Biol. 2025; 91: article number 70. https://doi.org/10.1007/s00285-025-02299-6

[15] Shafqat R, Abuasbeh K, Trabelsi S, Balti M. Epidemic dynamics prediction using fractional SIRD and deep learning. Sci Rep. 2026; 16: article number 3040. https://doi.org/10.1038/s41598-025-34299-3

[16] Ongun MY. The Laplace Adomian decomposition method for solving a model for HIV infection of CD4+ T cells. Math Comput Model. 2011; 53(5-6): 597-603. https://doi.org/10.1016/j.mcm.2010.09.009

[17] Haq F, Shah K, Rahman GU, Shahzad M. Numerical solution of fractional order smoking model via Laplace Adomian decomposition method. Alex Eng J. 2018; 57(2): 1061-9. https://doi.org/10.1016/j.aej.2017.02.015

[18] Baleanu D, Aydogn SM, Mohammadi H, Rezapour S. On modelling of epidemic childhood diseases with the Caputo-Fabrizio derivative. Alex Eng J. 2020; 59(5): 3029-39. https://doi.org/10.1016/j.aej.2020.05.007

[19] González-Gaxiola O, Biswas A. Optical solitons with Radhakrishnan-Kundu-Lakshmanan equation by Laplace-Adomian decomposition method. Optik. 2019; 179: 434-42. https://doi.org/10.1016/j.ijleo.2018.10.173

[20] Edeki SO, Motsepa T, Khalique CM, Akinlabi GO. Asian option pricing model via Laplace Adomian decomposition method. Open Phys. 2018; 16(1): 780-5. https://doi.org/10.1515/phys-2018-0097

[21] Naghipour A, Manafian J. Laplace Adomian decomposition for Burgers' equation. TWMS J Pure Appl Math. 2015; 6(1): 68-77.

[22] González-Gaxiola O, Biswas A. Chen-Lee-Liu equation by Laplace-Adomian decomposition method. Opt Quantum Electron. 2018; 50: 1-11. https://doi.org/10.1007/s11082-018-1583-0

[23] Paul S, Mondal SP, Bhattacharya P. Lotka-Volterra model via numerical methods. Alex Eng J. 2016; 55(1): 613-7. https://doi.org/10.1016/j.aej.2015.12.026

[24] Günerhan H, Kaabar MKA, Çelik E. Fractional smoking model. Sigma J Eng Nat Sci. 2023; 41: 331-43.

[25] Günerhan H, Dutta H, Dokuyucu MA, Adel W. Fractional HIV model. Chaos Solitons Fractals. 2020; 139: 110053. https://doi.org/10.1016/j.chaos.2020.110053

[26] Günerhan H, Rezazadeh H, Adel W, Hatami M, Martin Sagayam K, Emadifar H. Analytical approximate solution of fractional order smoking epidemic model. Adv Mech Eng. 2022; 14(9): 1-11. https://doi.org/10.1177/16878132221123888

[27] Adel W, Günerhan H, Nisar KS, Agarwal P, El-Mesady A. Fractional COVID-19 model. Sci Rep. 2024; 14: 2926. https://doi.org/10.1038/s41598-023-50889-5

[28] Hariharan S, Manimaran J, Shangerganesh L. Fractional SIR model stability. Rocky Mt J Math. 2025; 55(1): 211-25. https://doi.org/10.1216/rmj.2025.55.211

[29] Liu L, Jiang D, Hayat T. SIR model with regime switching. Physica A. 2021; 574: 125992. https://doi.org/10.1016/j.physa.2021.125992

[30] Alkahtani BST, Alzaid SS. COVID-19 fractional model. Chaos Solitons Fractals. 2020; 138: 110006. https://doi.org/10.1016/j.chaos.2020.110006

[31] Sefidgar E, Celik E, Shiri B. HIV fractional model. Int J Appl Math Stat. 2017; 56: 23-32.

[32] Caputo M. Linear models of dissipation whose Q is almost frequency independent-II. Geophys J R Astron Soc. 1967; 13: 529-39. https://doi.org/10.1111/j.1365-246X.1967.tb02303.x

[33] Li C, Qian D, Chen YQ. On Riemann-Liouville and Caputo derivatives. Discrete Dyn Nat Soc. 2011; 2011: 562494. https://doi.org/10.1155/2011/562494